ACS Macro Letters

pubs.acs.org/macroletters Letter

Elasticity and Viscosity of DNA Liquid Crystals

Liana Lucchetti, Tommaso P. Fraccia, Giovanni Nava, Taras Turiv, Fabrizio Ciciulla, Lucas Bethge, Sven Klussmann, Oleg D. Lavrentovich, and Tommaso Bellini*

Cite This: ACS Macro Lett. 2020, 9, 1034−1039 Read Online

ACCESS | Metrics & More | Article Recommendations | Supporting Information

ABSTRACT: Concentrated solutions of blunt-ended DNA oligomer duplexes self-assemble in living polymers and order into lyotropic nematic liquid crystal phase. Using the optical torque provided by three distinct illumination geometries, we induce independent splay, twist, and bend deformations of the DNA nematic and measure the corresponding elastic coefficients K_1, K_2, and K_3, and viscosities η_{splay}, η_{twist}, and η_{bend}. We find the viscoelasticity of the system to be remarkably soft, as the viscoelastic coefficients are smaller than in other lyotropic liquid crystals. We find $K_1 > K_3 > K_2$, in agreement with the elasticity of the nematic phase of flexible polymers, and $\eta_{bend} > \eta_{splay} > \eta_{twist}$ a behavior that is nonconventional in the context of chromonic, polymeric, and thermotropic liquid crystals, indicating a possible role of the weakness and reversibility of the DNA aggregates.

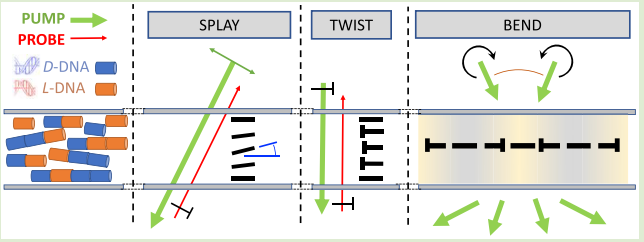

Lyotropic liquid crystals (LC) are a large family of structured fluid materials of different built and nature, whose rheology and elasticity are only partially known. Investigating their mechanical properties is both a route toward innovation and a opening for a better understanding of their often rich dynamic microscopic structure. We focus here on the viscoelasticity of oligo-DNA LCs, a class of lyotropic liquid crystalline materials in which long-range LC ordering emerges via three-step self-assembly: hybridization of DNA oligomers into duplexes whose axial ratio depends on the oligomer length, their linear aggregation via end-to-end stacking, and their ordering into nematic LC phases (see sketches in Figure 1a−c).[1] Because of their structure, oligo-DNA LCs share characters of chromonic and polymeric lyotropic LC, two classes of materials whose viscoelastic properties are markedly different from those of thermotropic LC and still miss a full molecular interpretation. Analogously to chromonic LC, ordering in oligo-DNA is based on the columnar stacking of monomers, which in the case of chromonics are flat polycyclic molecules, while in oligo-DNA are cylindrical-like duplexes. In oligo-DNA, the height-to-diameter ratio of the monomers is much larger, and the stacking energy is much weaker than in chromonics,[2,3] yielding a significant flexibility of the linear aggregates, a feature known to deeply affect the viscoelasticity of polymeric LCs such as polybenzylglutamate (PBG).[4]

While the thermodynamics of oligoDNA LCs have been characterized and modeled,[1,5−9] their viscoelasticity is unknown because of a combination of difficulties: DNA LCs are intrinsically chiral[10] and problematic to align, making it difficult to use typical light-scattering-based analysis; moreover, their coupling with electric and magnetic fields, another

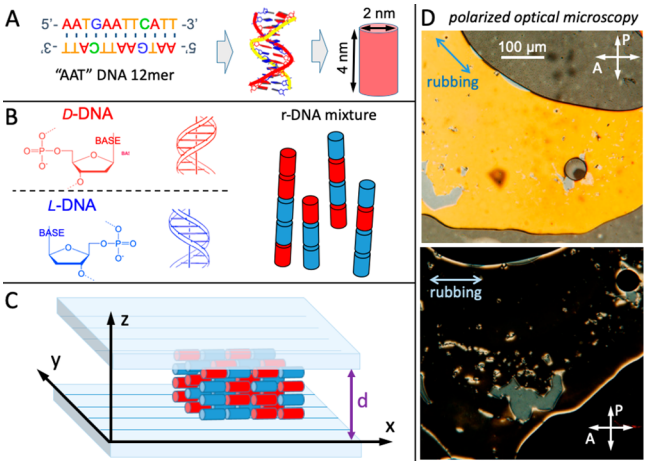

Figure 1. Sketch of the experimental conditions: (A) Palindromic 12mer "AAT" DNA sequence provides the formation of blunt-end duplexes, which can be schematized as cylinders with axial ratio ≈2; (B) Samples are obtained by an equimolar mixtures of D-DNA and L-DNA AAT sequences, which selectively hybridize into L and D duplexes (red and blue cylinders, respectively); (C) The racemic mixture is aligned by enclosing it between parallel photorubbed double-coated flat plates; (D) Polarized optical microscopy demonstrates the uniform alignment of the r-DNA domain, which appears bright or extinguished depending on the relative orientation of surface treatment and polarizers.

Received: May 22, 2020
Accepted: June 19, 2020
Published: June 24, 2020

https://dx.doi.org/10.1021/acsmacrolett.0c00394
ACS Macro Lett. 2020, 9, 1034−1039

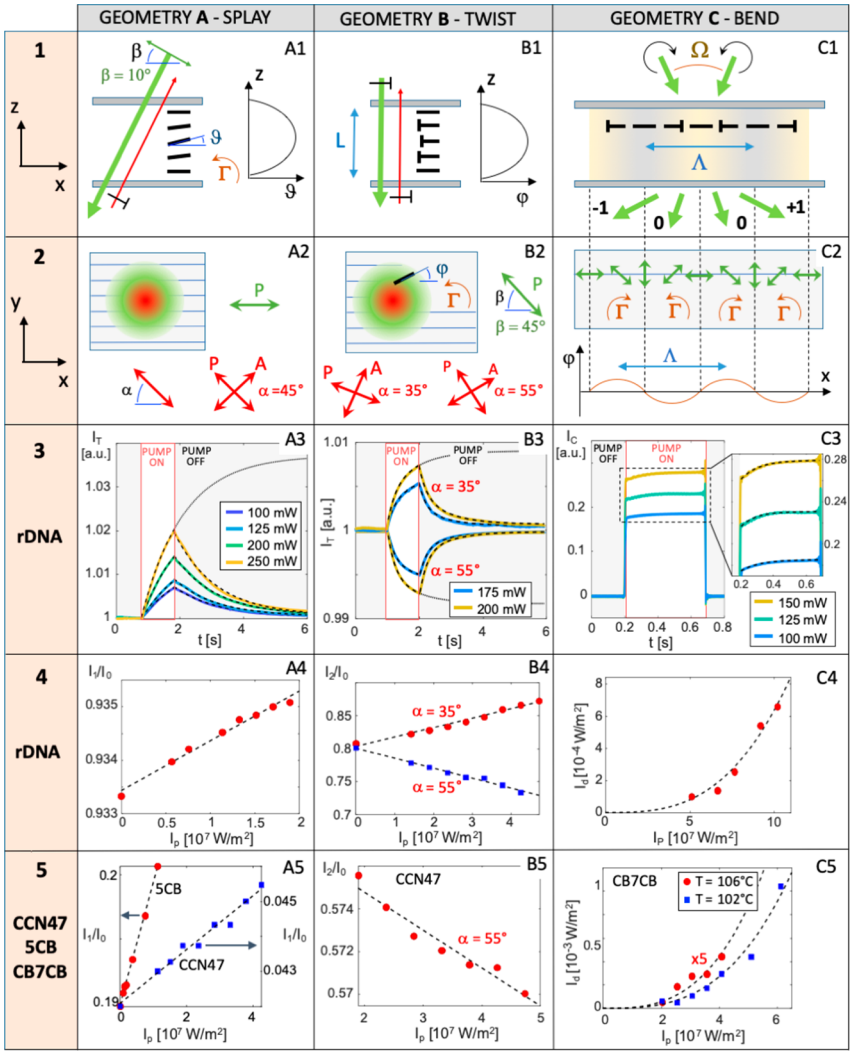

Figure 2. Experimental concept and data. Columns A−C describe experimental design and results for the three geometries, enabling all-optical determination of elastic coefficients and viscoelastic ratios. Rows 1 and 2: sketch of the x−z and x−y projections of the illumination geometries. Green and red lines and shades indicate the pump and the probe beams, respectively. Thick black segments (A1, B1): nematic director. Thin blue lines (A2, B2): rubbing direction. Definition of angles: between pump field and director (β, in A1 and B2), between probe field and director (α, in A2), between director and rubbing in the x−z plane (ϑ, in A1) and in the x−y plane (φ, in B2), between the two interfering pump beams (Ω, C2). L is the cell thickness (B1). Γ is the optical torque on the director, which is either in the x−z (A1) or in the x−y plane (B2, C2). Λ is the pitch of the polarization grating (C1). Row 3: measured probe (A3, B3) and self-diffracted intensities (C3) vs time. Colored lines: data for different pump intensity as in legend. Dashed black lines: exponential (A3, C3 and inset) and double exponential (B3) fitting lines, whose extrapolated values for long times (dotted line) give I_1 (A3) and I_2 (B3). Rows 4 and 5: stationary values of the probe (A3, B3) and self-diffracted intensity (C3) vs pump intensity I_p for rDNA (row 4) and thermotropic nematics (row 5). Dashed lines: best fit to the data with eq 3. CB7CB data for T = 106 °C (C5) are amplified five times for visualization.

standard strategy to investigate LC, is too weak. Here we overcome these difficulties and measure the three elastic coefficients and related viscosities by exploiting the combination of (i) an achiral oligo-DNA system; (ii) recently developed photoaligned surfaces; and (iii) the use of optical fields whose effectiveness in the context of oligo-DNA LCs was recently shown,[11] to couple to the nematic director in selected areas of a few tens of microns, which enables circumventing issues related to defects and impurities.

The chirality of oligo-DNA LCs can be suppressed by stoichiometric balance of "natural" right-handed oligomers with their enantiomer.[12] Here we study a racemic DNA mixture ("r-DNA") of 12-base-long oligomers (5′-AAT-GAATTCATT-3′, "AAT") obtained by solid-state synthesis with Na as counterion. Being AAT molecules self-complementary, once in water they readily hybridize to form an equal number of right- and left-handed blunt-ended duplexes (Figure 1A).[12] We find that the resulting achiral nematic phase can be homogeneously aligned by sandwiching it between two parallel multilayer photoaligned substrates recently developed for chromonic LCs[13] (Figure 1C,D and SI). We performed experiments at room temperature on L = 15 μm thick cells filled by r-DNA at a concentration ≈500 mg/mL (a figure to be compared with the density ≈1800 mg/mL of lyophilized DNA) and no added salt, at which the fluid is a nematic with birefringence $\Delta n \approx -0.025$. Ancillary control measurements have been performed on the thermotropic LCs 5CB (4-pentyl-4-cyanobiphenyl), CCN47 (4′-butyl-4-heptyl-bicyclohexyl-4-carbononitrile), and CB7CB (1,7-bis-4-(4-cyanobiphenyl)-heptane; see SI).

https://dx.doi.org/10.1021/acsmacrolett.0c00394
ACS Macro Lett. 2020, 9, 1034−1039

Probing LC elasticity with external forces is an approach extensively used since the early 1970s. Here we revisit that approach by using optical forces, whose flexibility enabled us to design three distinct torque geometries (Figure 2, columns A–C) that selectively induce splay, twist, and bend. In all geometries, samples are irradiated by a pump beam of intensity I_p providing a torque density

$$\Gamma = \frac{\Delta n}{c} I_p \sin 2\beta \tag{1}$$

where β is the angle of the optical field E with the rubbing direction (x) and c is the speed of light. Experiments were performed by stepwise irradiation of the samples by an Ar^+ laser (λ = 514 nm, $I_p = 10^4$–10^7 W/m^2).

In Geometry A, the pump beam has oblique incidence and polarization in the x–z plane. The resulting Γ induces a tilt $\vartheta(z)$ of the director $\mathbf{n}$ in the x–z plane, which corresponds to a pure splay deformation. This is sketched in Figure 2A1, where we assume $\Delta n < 0$ as for DNA and CCN 47. This deformation is detected by a low power probe beam (a 5 mW HeNe laser) of intensity I_0, counter-propagating with respect to the pump, focused at the center of the pump spot, and linearly polarized at 45° with respect to the pump beam (Figure 2A2). The transmitted intensity I_T is measured after the probe beam passes a crossed analyzer. As the splay deformation is induced, the effective birefringence experienced by the probe beam changes, producing a variation in the transmitted intensity. This can be appreciated in Figure 2A3, where we plot the response of the r-DNA cell to the turning on and off of the pump field for different pump powers (colored lines). We fit all $I_T(t)$ with exponential rises and decays having equal characteristic times (dashed lines). The saturation values I_1 of the fitting functions, normalized by I_0, are shown versus I_p in Figure 2A4 for rDNA and in Figure 2A5 for 5CB and CCN47.

Geometry B is instead designed to produce a deformation of pure twist. In this case, the cell is illuminated with both pump and probe normal to the cell surface. The polarization of the pump beam is at 45° with respect to the rubbing direction, thus producing a torque and an angular deformation $\varphi(z)$ in x–y plane, sketched in Figure 2B1,B2 for $\Delta n < 0$. The probe beam is linearly polarized at an angle α which is either 35° or 55° degrees to cell rubbing and measured after a crossed analyzer. As the twist deformation is induced, $\mathbf{n}$ is tilted away from the rubbing direction, producing an increase or decrease in the transmitted intensity I_T, depending on α. This is shown in Figure 2B3, where we plot I_T versus time for rDNA for α = 35° and α = 55° and different values of I_p (colored lines). We fit all $I_T(t)$, rise and fall, with equal double exponentials (same characteristic times and relative intensities, dashed lines), from which we determine the saturation values I_2. Figure 2B4 and B5 show I_2/I_0 versus I_p for rDNA and CCN47, respectively.

Geometry C is aimed at inducing a bend deformation by exploiting a polarization grating. This is realized by superimposing two beams with equal intensity and circular polarizations of opposite handedness (Figure 2C1). The resulting field is linearly polarized, with the angle between polarization and x axis continuously rotating in x, as sketched in Figure 2C2. The period of such rotation is $\Lambda = \lambda_0/(2 \sin(\Omega_0/2))$, where Ω_0 is the angle between the two beams in air. The resulting torque induces a periodic deformation $\varphi(x)$ of pitch Λ, which acts as a phase grating producing self-diffraction. We measure the intensity of the first self-diffraction order to quantify the bend deformation. Indeed, since Λ is much smaller than the cell thickness, the deformation is approximately of pure bend (see SI). Figure 2C3 shows I_C, the intensity measured in the position of the first self-diffraction order for various I_p (colored lines). The diffracted intensity I_d can be extracted from the saturation values of the exponential fits to $I_C(t)$ (dashed lines) after correcting for the scattered pump light as detailed in the SI. I_d versus I_p is reported in Figure 2C4 for rDNA and Figure 2C5 for CB7CB.

The perturbations of the director (ϑ and φ for tilt in the xz and xy plane, respectively) reach an equilibrium when optical and elastic torque densities are balanced, selectively involving, in the three geometries, the three elastic coefficients: $\tau_{OPT} = K_1 \frac{d^2\vartheta}{dz^2}$, $\tau_{OPT} = K_2 \frac{d^2\varphi}{dz^2}$, $\tau_{OPT} \approx K_3 \frac{4\pi^2}{\Lambda^2}\varphi(x, z)$. The resulting perturbation in the nematic direction is, in the three cases:

$$\vartheta(z) = \left(\frac{\Delta n I_p \sin 2\beta}{2cK_1}\right)\left(\frac{L^2}{4}\right)\left(\frac{4z(L-z)}{L^2}\right),$$

$$\varphi(z) = \left(\frac{\Delta n I_p}{2cK_2}\right)\left(\frac{L^2}{4}\right)\left(\frac{4z(L-z)}{L^2}\right),$$

$$\varphi(x) \approx \left(\frac{\Delta n I_p}{2cK_3}\right)\left(\frac{\Lambda^2}{2\pi^2}\right)\left(\sin\frac{2\pi x}{\Lambda}\right) \tag{2}$$

where the terms in the first parenthesis express the optical-to-elastic balance, those in the second parenthesis give the dependence on the characteristic length of the perturbation, while those in the third are $[-1,1]$-bounded functions expressing the spatial dependence. The orientational perturbations in eq 2, whose dependence on z, I_p, and K are as expected for a nematic under the action of a uniform field,[14] are in fact oversimplified, as they are obtained in the assumption that the cell thickness is small enough that the polarization of the pump beam is maintained throughout the cell. Despite the thinness of the cell and the low birefringence of oligoDNA-LC, this condition is partly violated. Thus, the second and the third of eqs 2 need to be corrected modifying the blue terms as described in the SI. From eq 2, with corrections included, we can compute the expected dependence of the optical signals on K_1, K_2, and K_3. At the lowest order in the director perturbation we obtain, as expected based on symmetry,

$$\frac{I_1}{I_0} = A_1 + \frac{B_1}{K_1} I_p, \quad \frac{I_2}{I_0} = A_2 + \frac{B_2}{K_2} I_p, \quad I_d = \frac{C_3}{K_3^2} I_p^3 \tag{3}$$

where the coefficients A_1, B_1, A_2, B_2, and C_3 are computed in the SI. The best fit to the data according to eq 3 are shown in Figure 2A4, B4, and C4 for r-DNA and Figure 2A5, B5, and C5 for thermotropic LCs.

Our measurements convey information on the system kinetics too, as apparent from the transient behavior shown in Figure 2A3, B3, and C3. Nematodynamic equation applied to Geometry A predicts exponential rise and decay relaxations with a characteristic time $\tau_1 = \eta_{splay} L^2/\pi^2 K_1$. Geometry B leads to a situation a bit more complex because of the modification in the pump polarization as it propagates in the cell. In this case, the relaxation of the director deformation is given by the sum of two exponentials since it involves a significant contribution from the next spatial mode, the two characteristic times being $\tau_{21} = \eta_{twist} L^2/\pi^2 K_2$ and $\tau_{22} = \tau_{21}/4$. In Geometry C, where the characteristic length of the deformation is Λ, we expect an exponential relaxation with the characteristic time τ_3

https://dx.doi.org/10.1021/acsmacrolett.0c00394
ACS Macro Lett. 2020, 9, 1034–1039

$= \eta_{bend}\Lambda^2/4\pi^2K_3$. The diffracted peak sits on a background of scattered intensity that abruptly appears as the pump beam is switched on. Thus, in the transient behavior, the exponential rise is added to a step function, as visible in Figure 2C3. The best fits of the kinetic behaviors are shown in Figure 2A3, B3, and C3 as dashed black lines. The quality of the fit is satisfactory in all cases.

The elastic coefficients and viscosities that we obtain for rDNA and thermotropic LCs are reported in Table 1 that also displays, for comparison, literature data for chromonic LCs (disodium cromoglycate, DSCG)[2] and LCs of flexible polymers (poly-γ-benzyl glutamate, PBG).[4] The results we obtain for thermotropic LCs are in good agreement with the literature (in italics).[2,15−19] Results for rDNA are a bit unconventional and need to be discussed.

Table 1. Elastic Coefficients and Viscosities of the Nematic Phase of rDNA, 5CB, CCN 47, CB7CB, and the chiral nematic phase of AAT[a]

	K_1 (pN)	K_2 (pN)	K_3 (pN)	η_{splay} (Pa·s)	η_{twist} (Pa·s)	η_{bend} (Pa·s)
rDNA	**1.7**	**0.4**	**0.9**	**0.10**	**0.03**	**0.19**
5CB[2,18,19]	**5.0** *(5.5)*	*(2.5)*	*(6.2)*	**0.09** *(0.09)*	*(0.10)*	*(0.02)*
CCN47[16,17]	**6.0** *(10)*	**1.1**		**0.12**	**0.15** *(0.2)*	
CB7CB[15] (T = 106 °C)			**0.45** *(0.55)*			**0.03** *(0.05)*
CB7CB[15] (T = 102 °C)			**0.14** *(0.40)*			**0.03** *(0.05)*
AAT DNA		**0.24**			**0.04**	
DSCG[2]	10.2	0.7	24.9	11.7	10.5	0.009
PBG[4]	7.5	0.6	6	2.5	2.5	0.025

[a]Bold numbers: data from this work. Italic numbers: data from literature (refs in superscript). The last two rows show literature data for the chromonic LC DSCG (volume fraction $\phi = 0.115$) and for the polymer LC PBG ($\phi = 0.16$). The estimated accuracy on the measured values is 20%.

Inspection of Table 1 reveals noticeable features of rDNA elasticity: (i) the elastic coefficients are smallest among all known types of nematic LCs; (ii) $K_1 > K_3 > K_2$, analogously to polymeric LCs, but differently from conventional thermotropic nematics for which $K_3 > K_1 > K_2$, as is generally the case also for chromonic LCs, with exceptions found at high concentration[2,3] and in the presence of divalent salts;[20] (iii) K_2 is much smaller than the other elastic constants, confirming the softness of twist modes to be a universal feature of lyotropic nematics. As a control, we measured K_2 of the chiral nematic phase of nonracemic AAT mixtures with the experimental approach of ref 11 and found a compatible value (see Table 1); (iv) $K_1/K_2 \sim 4$ is the smallest among lyotropic LCs (which typically show[2] $K_1/K_2 \sim 10$).

A possible key to understanding the observed behavior is in the combination, distinctive of oligo-DNA LCs, of moderate aggregate length L_a (∼ a few tens of monomers[8,9]) and short persistence length l_p, of the order of a few monomers, much shorter than the $l_p \approx 50$ nm of long DNA double strands, reflecting the equilibrium reconnection of the duplexes. Indeed, both L_a and l_p of oligo-DNA are shorter than those of chromonic LCs, as indicated by the larger minimum concentration for LC ordering (>300 mg/mL for oligo-DNA and ≈100 mg/mL for DSCG) despite the much larger axial ratio (2 for rDNA vs <0.2 for DSCG). This also agrees with the estimates for stacking energy ("scission energy"), weaker in oligo-DNA ($\sim 5k_BT$ [1]) than in chromonics ($\sim 10k_BT$ for DSCG[3]). Models for LCs formed by flexible rods,[2,4] indicate that, at any given volume fraction, the three elastic coefficients depend on L_a ($K_1 \propto L_a$) and on l_p ($K_2 \propto l_p^{1/3}$, $K_3 \propto l_p$). These scaling behaviors suggest that $K_3 < K_1$ is a consequence of the flexibility of oligo-DNA aggregates, while the general soft elasticity of oligo-DNA reflects the small values of L_a and l_p. We speculate that such intrinsic softness is further increased by the simple DNA LC structure, a consequence of duplex geometry and weak aggregation, which prevents the formation of entangled, bundled, and branched structures that might stiffen, to some degree, chromonic and polymer LCs.

The viscosities of rDNA are strongly nonconventional since $\eta_{bend} > \eta_{splay} > \eta_{twist}$, with η_{splay} and η_{twist} smaller than in other LC material. In thermotropic LCs, $\eta_{twist} > \eta_{bend} > \eta_{splay}$. In lyotropic polymers and chromonic materials, $\eta_{splay} \geq \eta_{twist} > \eta_{bend}$[2]. We confirmed the value of twist viscosity with the approach of ref 11 on nonracemic AAT (see Table 1 and SM). We speculate that the thinness of this system is intimately related to its softness. Indeed, the weak, easily reversible interduplex bonds must have a dynamic counterpart in their short lifetime. We thus envision the oligo-DNA nematics as a highly dynamic system, where the ordering is in large part provided by the molecular packing, a situation markedly different from chromonic nematics. We speculate that the easy breaking and recombination of DNA aggregates in the absence of bifurcations and entanglements lead to the observed significant fluidity. This notion agrees with the observed exception of bend, a deformation that best preserves the local columnar packing and, thus, is the least prone to relax via recombination. It is worth noticing that the theoretical approach based on the Leslie coefficients leading to the notion that η_{twist} has to be the largest viscosity, is based on the assumption of incompressible nematics,[14] which might not be transferable to systems with significant osmotic compressibility, such as lyotropic LCs. Interestingly, η_{twist} smaller than other viscosities has recently been observed in a bent-core nematic[21] and tentatively attributed to the formation of local supramolecular structures.

OligoDNA-LC has unique features: it is a natural molecule, it has a multilevel hierarchical self-assembly, it undergoes LC ordering, and as here demonstrated, is the softest and thinnest LC fluid. Through its viscoelastic behavior, oligoDNA LC emerges as a lyotropic system of its own kind, different from both chromonic and polymeric LCs. Our findings emphasize the need for a broader theoretical understanding of the mechano-elastic properties of nematic fluids capable of encompassing the continuously expanding variety of self-assembled systems.

■ ASSOCIATED CONTENT

Supporting Information

The Supporting Information is available free of charge at https://pubs.acs.org/doi/10.1021/acsmacrolett.0c00394.

Detailed information on preparation of the aligning substrates, description of the models used for data interpretation, information on measurements on thermotropic LC used as tests (PDF)

https://dx.doi.org/10.1021/acsmacrolett.0c00394
ACS Macro Lett. 2020, 9, 1034−1039

AUTHOR INFORMATION

Corresponding Author

Tommaso Bellini − *Dipartimento di Biotecnologie Mediche e Medicina Traslazionale, Università di Milano, I-20090 Segrate, MI, Italy;* orcid.org/0000-0003-4898-4400; Email: tommaso.bellini@unimi.it

Authors

Liana Lucchetti − *Dipartimento SIMAU, Università Politecnica delle Marche, 60131 Ancona, Italy*

Tommaso P. Fraccia − *Institute Pierre-Gilles de Gennes, CBI UMR8231, ESPCI Paris-CNRS, PSL Research University, 75005 Paris, France; Dipartimento di Biotecnologie Mediche e Medicina Traslazionale, Università di Milano, I-20090 Segrate, MI, Italy;* orcid.org/0000-0002-9638-4269

Giovanni Nava − *Dipartimento SIMAU, Università Politecnica delle Marche, 60131 Ancona, Italy; Dipartimento di Biotecnologie Mediche e Medicina Traslazionale, Università di Milano, I-20090 Segrate, MI, Italy*

Taras Turiv − *Advanced Materials and Liquid Crystal Institute, Chemical Physics Interdisciplinary Program, Kent State University, Kent, Ohio 44242, United States*

Fabrizio Ciciulla − *Dipartimento SIMAU, Università Politecnica delle Marche, 60131 Ancona, Italy;* orcid.org/0000-0001-7746-7221

Lucas Bethge − *NOXXON Pharma AG, 10589 Berlin, Germany*

Sven Klussmann − *NOXXON Pharma AG, 10589 Berlin, Germany*

Oleg D. Lavrentovich − *Advanced Materials and Liquid Crystal Institute, Chemical Physics Interdisciplinary Program and Department of Physics, Kent State University, Kent, Ohio 44242, United States;* orcid.org/0000-0002-0128-0708

Complete contact information is available at: https://pubs.acs.org/10.1021/acsmacrolett.0c00394

Author Contributions

The manuscript was written with the contribution of all authors. All authors have given approval to the final version of the manuscript.

Funding

T.B. acknowledges support by PRIN2017 Project from Ministero Istruzione, Università e Ricerca [ID 2017Z55KCW].

Notes

The authors declare no competing financial interest.

ACKNOWLEDGMENTS

Authors are grateful to Fulvio Bisi, Alberta Ferrarini, Victor Reshetnyak, Francesco Simoni, and Giuliano Zanchetta for useful discussions and to Simone Di Leo for help in the cell preparations.

REFERENCES

(1) Nakata, M.; Zanchetta, G.; Chapman, B. D.; Jones, C. D.; Cross, J. O.; Pindak, R.; Bellini, T.; Clark, N. A. End-to-End Stacking and Liquid Crystal Condensation of 6-to 20-Base Pair DNA Duplexes. *Science (Washington, DC, U. S.)* **2007**, *318* (5854), 1276−1279.

(2) Zhou, S.; Neupane, K.; Nastishin, Y. A.; Baldwin, A. R.; Shiyanovskii, S. V.; Lavrentovich, O. D.; Sprunt, S. Elasticity, Viscosity, and Orientational Fluctuations of a Lyotropic Chromonic Nematic Liquid Crystal Disodium Cromoglycate. *Soft Matter* **2014**, *10* (34), 6571−6581.

(3) Zhou, S.; Nastishin, Y. A.; Omelchenko, M. M.; Tortora, L.; Nazarenko, V. G.; Boiko, O. P.; Ostapenko, T.; Hu, T.; Almasan, C. C.; Sprunt, S. N.; Gleeson, J. T.; Lavrentovich, O. D. Elasticity of Lyotropic Chromonic Liquid Crystals Probed by Director Reorientation in a Magnetic Field. *Phys. Rev. Lett.* **2012**, *109* (3), na.

(4) Lee, S. D.; Meyer, R. B. Crossover Behavior of the Elastic Coefficients and Viscosities of a Polymer Nematic Liquid Crystal. *Phys. Rev. Lett.* **1988**, *61* (19), 2217−2220.

(5) Fraccia, T. P.; Smith, G. P.; Bethge, L.; Zanchetta, G.; Nava, G.; Klussmann, S.; Clark, N. A.; Bellini, T. Liquid Crystal Ordering and Isotropic Gelation in Solutions of Four-Base-Long DNA Oligomers. *ACS Nano* **2016**, *10* (9), 8508−8516.

(6) Bellini, T.; Zanchetta, G.; Fraccia, T. P.; Cerbino, R.; Tsai, E.; Smith, G. P.; Moran, M. J.; Walba, D. M.; Clark, N. A. Liquid Crystal Self-Assembly of Random-Sequence DNA Oligomers. *Proc. Natl. Acad. Sci. U. S. A.* **2012**, *109* (4), 1110−1115.

(7) Zanchetta, G.; Bellini, T.; Nakata, M.; Clark, N. A. Physical Polymerization and Liquid Crystallization of RNA Oligomers. *J. Am. Chem. Soc.* **2008**, *130* (39), 12864−12865.

(8) De Michele, C.; Bellini, T.; Sciortino, F. Self-Assembly of Bifunctional Patchy Particles with Anisotropic Shape into Polymers Chains: Theory, Simulations, and Experiments. *Macromolecules* **2012**, *45* (2), 1090−1106.

(9) De Michele, C.; Rovigatti, L.; Bellini, T.; Sciortino, F. Self-Assembly of Short DNA Duplexes: From a Coarse-Grained Model to Experiments through a Theoretical Link. *Soft Matter* **2012**, *8* (32), 8388−8398.

(10) Zanchetta, G.; Giavazzi, F.; Nakata, M.; Buscaglia, M.; Cerbino, R.; Clark, N. A.; Bellini, T. Right-Handed Double-Helix Ultrashort DNA Yields Chiral Nematic Phases with Both Right- and Left-Handed Director Twist. *Proc. Natl. Acad. Sci. U. S. A.* **2010**, *107* (41), 17497−17502.

(11) Lucchetti, L.; Fraccia, T. P.; Ciciulla, F.; Bellini, T. Non-Linear Optical Measurement of the Twist Elastic Constant in Thermotropic and DNA Lyotropic Chiral Nematics. *Sci. Rep.* **2017**, *7* (1), na.

(12) Rossi, M.; Zanchetta, G.; Klussmann, S.; Clark, N. A.; Bellini, T. Propagation of Chirality in Mixtures of Natural and Enantiomeric Dna Oligomers. *Phys. Rev. Lett.* **2013**, *110* (10), na.

(13) Peng, C.; Guo, Y.; Turiv, T.; Jiang, M.; Wei, Q. H.; Lavrentovich, O. D. Patterning of Lyotropic Chromonic Liquid Crystals by Photoalignment with Photonic Metamasks. *Adv. Mater.* **2017**, *29* (21), 1606112.

(14) DeGennes, P. G.; Prost, J. *The Physics of Liquid Crystals*; Clarendon Press: Oxford, 1993.

(15) Babakhanova, G.; Parsouzi, Z.; Paladugu, S.; Wang, H.; Nastishin, Y. A.; Shiyanovskii, S. V.; Sprunt, S.; Lavrentovich, O. D. Elastic and Viscous Properties of the Nematic Dimer CB7CB. *Phys. Rev. E: Stat. Phys., Plasmas, Fluids, Relat. Interdiscip. Top.* **2017**, *96* (6), na.

(16) Zawadzki, A.; Walton, H. G. Measurements of the Splay and Bend Elastic Constants of 4′-Butyl-4-Heptyl-Bicyclohexyl-4-Carbononitrile, CCN47. *Mol. Cryst. Liq. Cryst.* **2012**, *569* (1), 10−14.

(17) Praveen Kumar, M.; Venkata Sai, D.; Dhara, S. Effect of Sm- A Short-Range Order on the Activation Energies of Translational and Rotational Viscosities of Nematic Liquid Crystals with Highly Polar Molecules. *Phys. Rev. E: Stat. Phys., Plasmas, Fluids, Relat. Interdiscip. Top.* **2018**, *98* (6), na.

(18) Chmielewski, A. G. Viscosity Coefficients of Some Nematic Liquid Crystals. *Mol. Cryst. Liq. Cryst.* **1986**, *132* (3−4), 339−352.

(19) Cui, M.; Kelly, J. R. Temperature Dependence of Visco-Elastic Properties of 5CB. *Mol. Cryst. Liq. Cryst. Sci. Technol., Sect. A* **1999**, *331* (1), 49−57.

(20) Zhou, S.; Cervenka, A. J.; Lavrentovich, O. D. Ionic-Content Dependence of Viscoelasticity of the Lyotropic Chromonic Liquid Crystal Sunset Yellow. *Phys. Rev. E - Stat. Nonlinear, Soft Matter Phys.* **2014**, *90* (4), na.

(21) Majumdar, M.; Salamon, P.; Jákli, A.; Gleeson, J. T.; Sprunt, S. Elastic Constants and Orientational Viscosities of a Bent-Core

Nematic Liquid Crystal. *Phys. Rev. E - Stat. Nonlinear, Soft Matter Phys.* **2011**, *83* (3), na.

https://dx.doi.org/10.1021/acsmacrolett.0c00394
ACS Macro Lett. 2020, 9, 1034−1039